Microvascular Research 60, 149–159 (2000)
doi:10.1006/mvre.2000.2255, available online at http://www.idealibrary.com on IDEAL®

Formation and Actions of Cyclic ADP-Ribose in Renal Microvessels

Ningjun Li, Eric G. Teggatz, Pin-Lan Li, Roxanne Allaire, and Ai-Ping Zou

Departments of Physiology and Pharmacology & Toxicology, Medical College of Wisconsin, Milwaukee, Wisconsin 53226

Received February 4, 2000

Recent studies indicated that cyclic ADP-ribose (cADPR) serves as a second messenger for intracellular Ca^{2+} mobilization in a variety of mammalian cells. However, the metabolism and actions of cADPR in the renal vasculature are poorly understood. In the present study, we characterized the enzymatic pathway of the production and metabolism of cADPR along the renal vascular tree and determined the role of cADPR in the control of intracellular [Ca^{2+}] and vascular tone. The high performance liquid chromatographic analyses showed that cADPR was produced and hydrolyzed along the renal vasculature. The maximal conversion rate of nicotinamide guanine dinucleotide (NGD) into cyclic GDP-ribose (that represents ADP-ribosyl cyclase activity for cADPR formation) was 8.69 ± 2.39 nmol/min/mg protein in bulk-dissected intrarenal preglomerular vessels ($n = 7$) and 4.35 ± 0.13, 2.23 ± 0.27, 2.40 ± 0.19, and 0.31 ± 0.02 nmol/min/mg protein, respectively, in microdissected arcuate arteries ($n = 6$), interlobular arteries ($n = 6$), afferent arterioles ($n = 7$), and vasa recta ($n = 10$). The activity of cADPR hydrolase was also detected in the renal vasculature. Using the fluorescence microscopic spectrometry, cADPR was found to produce a large rapid Ca^{2+} release from ***β***-escin-permeabilized renal arterial smooth muscle cells (SMCs). In isolated, perfused, and pressurized small renal arteries, cADPR produced a concentration-dependent vasoconstriction when added into the bath solution. The vasoconstrictor effect of cADPR was completely blocked by tetracaine, a Ca^{2+}-induced Ca^{2+} release (CICR) inhibitor. These results suggest that an enzymatic pathway for cADPR production and metabolism is present along the renal vasculature and that cADPR may importantly contribute to the control of renal vascular tone through CICR.

Key Words: cyclic ADP-ribose; calcium mobilization; Ca^{2+}-induced Ca^{2+} release; ADP-ribosyl cyclase; renal artery; kidney.

INTRODUCTION

Cyclic ADP-ribose (cADPR) is an endogenous metabolite of nicotinamide adenine dinucleotide (NAD) via ADP-ribosyl cyclase (Galione, 1993; Lee, 1994; Lee *et al.*, 1994). cADPR was first reported to be present in sea urchin eggs and to possess Ca^{2+}-mobilizing activity (Lee *et al.*, 1989). Recent studies have indicated that cADPR may be detected in a variety of mammalian tissues or cells such as heart, liver, spleen, brain tissues and red blood cells, lymphocytes, pituitary cells, and renal epithelial cells (Beer *et al.*, 1995b; Koshiyama *et al.*, 1991; Lee and Arthus, 1993; Takesawa *et al.*, 1993; White *et al.*, 1993). Tissue concentrations of cADPR in cardiac muscle, liver, and brain have been estimated as 100–200 nM (Galione, 1992; Lee *et al.*, 1994). The enzymes responsible for the synthesis and degrada-

0026-2862/00 $35.00

tion of this nucleotide have been characterized. In mammalian tissues, ADP-ribosyl cyclase is a membrane-bound enzyme. The reaction catalyzed by ADP-ribosyl cyclase does not require any exogenous cofactor (Lee, 1994). The enzyme responsible for the hydrolysis of cADPR is also membrane-bound and present in a wide range of mammalian tissues. This cADPR hydrolase catalyzes the hydrolysis of cADPR to produce ADPR (Galione, 1993; Lee, 1994).

It has been demonstrated that *Aplysia* ADP-ribosyl cyclase gene has 69% homology with human lymphocyte differentiate antigen CD38 (States *et al.*, 1992). Purified or recombinant human lymphocyte antigen CD38 protein and its mouse and rat homologue have been revealed to have both ADP-ribosyl cyclase and cADPR hydrolase activity (Howard *et al.*, 1993; Koguma *et al.*, 1994; Lee, 1994; Shubinsky and Schlesinger, 1997). This membrane-bound CD38 protein has been considered as a multiple functional enzyme to serve as a molecular switch for regulating the cellular levels of cADPR in mammalian tissues. The cellular cADPR levels could be elevated or decreased by balancing the synthetic and hydrolytic activities of CD38, respectively (Lee, 1994; Lee *et al.*, 1994). Recent studies in our laboratory have demonstrated that this enzymatic pathway responsible for the production and metabolism of cADPR is present in coronary arterial smooth muscle cells and that tissue cADPR concentration in coronary arterial smooth muscle is about 150 nM (Geiger *et al.*, 2000; Li *et al.*, 1998).

Cyclic ADPR produces intracellular Ca^{2+} mobilization in a variety of tissues and cells by a mechanism completely independent of *D-myo*-inositol 1,4,5-triphosphate (IP_3), since IP_3 receptor antagonist, heparin can not block the effect of cADPR (Galione, 1993; Lee, 1994; Lee *et al.*, 1994). It has been found to activate ryanodine receptors on the sarcoplasmic or endoplasmic reticulum and result in Ca^{2+} release (Galione, 1993; Lee *et al.*, 1994). There is increasing evidence indicating that cADPR serves as a second messenger to mediate the effects of a number of agonists to mobilize intracellular Ca^{2+} in different tissues or cells. Studies using pancreatic β cells strongly suggested that cADPR mediates glucose-induced insulin secretion (Takesawa *et al.*, 1993). cADPR may also mediate the effects of acetylcholine receptors in adrenal chromaffin cells, estrogen receptors on the uterus, 5-HT 2B receptor in arterial endothelial cells, and retinoic acid in renal tubular cells and aortic smooth muscle (Beers *et al.*, 1995b; Chini *et al.*, 1997, 1995; Morita *et al.*, 1997; Ullmer *et al.*, 1996).

In addition to these actions in mediating agonist responses, cADPR has been indicated to modulate Ca^{2+}-induced Ca^{2+} release (CICR), thereby regulating global Ca^{2+} levels within the cells (Galione *et al.*, 1991, 1998; Lee, 1993). The sensitization of ryanodine receptors by cADPR plays an important role in excitation-contraction coupling in cardiac muscle and in coupling between Ca^{2+} influx and intracellular Ca^{2+} release in the neurons. This CICR is of importance in the control of vascular tone, since the entry of Ca^{2+} through voltage-operating channels would produce a global Ca^{2+} increase throughout the cytoplasma and nucleus by CICR and thereby lead to vasoconstriction (Berridge, 1994, 1997; Galione *et al.*, 1998). cADPR may be involved in this amplification of intracellular Ca^{2+} signal through CICR. However, this hypothesis has to be tested. The role of cADPR-mediated Ca^{2+} signaling pathway in the control of vascular tone is poorly understood. The purpose of the present study was to characterize the enzymatic pathway of cADPR formation and metabolism in the renal vasculature, including renal pre- and postglomerular microvessels, using HPLC analysis and to examine the effect of cADPR on intracellular [Ca^{2+}] in renal arterial smooth muscle cells using fluorescent microscopic spectrometry. We also examined the effect of cADPR on the vascular tone using an isolated, perfused, and pressurized small renal arterial preparation and determined the contribution of CICR to cADPR-induced intracellular Ca^{2+} release and vasoconstriction.

MATERIALS AND METHODS

Preparation of the homogenates from bulk-dissected intrarenal arteries. Small intrarenal arteries were dissected as we described previously (Zou *et al.*, 1996a,b). Briefly, Sprague–Dawley rats weighing between 250 and 300 g were anesthetized with sodium pentobarbital (80 mg/kg body wt., i.p.), and the kid-

neys were flushed with physiological salt solution (PSS), which contains (mM): NaCl, 135; KCl, 3; $CaCl_2$, 1.5; $MgSO_4$, 1; KH_2PO_4, 2; Glucose 5.5; and Hepes, 5 (pH 7.4) and then perfused with 3% Evans blue in PSS. The kidneys were rapidly removed, placed in ice-cold PSS, and cut into 200-μm-thick sections. The tissue slices were incubated for 30 min in 2 ml of a low Ca^{2+} PSS (0.1 mM $CaCl_2$) containing 1 mg/ml of collagenase (type II, Worthington Biochem, Co.). Preglomerular arteries or arterioles that were filled with Evans blue were identified and collected under a Leica MZ8 stereomicroscope. The dissected arteries were homogenized with a glass homogenizer in ice-cold Hepes buffer, which contains (mM): Na-Hepes, 25; EDTA, 1; phenylmethylsulfonyl fluoride (PMSF), 0.1. After centrifugation of the homogenate at 6000g for 5 min at 4°C, the supernatant containing membrane and cytosolic components, termed homogenate, were frozen in liquid N_2 and stored at −80°C until used.

Microdissection of renal microvessels. Microdissection was performed as we described previously (Wu *et al.,* 1999). Sprague–Dawley rats were anesthetized with sodium pentobarbital, and the aorta below left renal artery was isolated and cannulated. After ligating the aorta at a site between the origin of the left and right renal arteries, the left kidney was flushed with 20 ml ice-cold dissection solution which contains (mM): NaCl, 135; KCl, 3; $CaCl_2$, 1.5; $MgSO_4$, 1; KH_2PO_4, 2; Glucose, 5.5; l-Alanine, 5; and Hepes, 5 (pH 7.4). Then the kidney was perfused with 1 ml blue polyethylene beads (diameter = 0.2 μm) for visualization of the renal microvessels. Following perfusion, the kidney was removed and cut into 1- to 2-mm-thick sections containing the entire corticomedullary axis. The sections were incubated at 37°C for 30 min in the digestion solution (1 mg/ml collagenase, 1 mg/ml dithiothreitol, and 1 mg/ml bovine albumin in dissection solution) with gentle shaking. During incubation, the samples were bubbled with a 95% O_2–5% CO_2 mixture. The sections were then rinsed twice with collagenase-free dissection solution and transferred into Petri dishes filled with ice-cold dissection solution containing 0.1 mg/ml trypsin inhibitor and 20 μg/ml aprotinin. A petri dish was mounted on the microscope stage and maintained at 4°C during dissection. Microdissection was performed under a Leica MZ8 stereomicroscope with dark-field illumination. The renal vascular and tubule segments and glomeruli were dissected, including arcuate artery (ArA), interlobular artery (IA), afferent arteriole (AA), vasa recta (VR), proximal convoluted tubule (PCT), and medullary collecting duct (mTAL). These vascular and tubular segments were recognized based on their unique feature under microscope as described previously (Wu *et al.*, 1999). To differentiate the afferent and efferent arterioles, the glomeruli attached to both afferent arterioles and interlobular arteries were chosen, and then the afferent arterioles were dissected from glomeruli and interlobular arteries. Seventy percent of these glomeruli had efferent arterioles attached, which were not attached to Evans blue-stained interlobular arteries. The length of these segments was measured with a calibrated eyepiece micrometer, and the glomeruli (Glm) were counted under microscope. Microdissected vessels, tubules, and glomeruli were lysed in 0.15 M sodium phosphate buffer solution and sonicated for 15 s, three times at 45 W using a microsonicator. The time period for dissection was limited to 1.5 h. In general, 20 glomeruli and 10- to 20-mm vascular and tubular segments were pooled to use as one sample for the analysis of the enzyme activity and assay of protein concentrations. The protein concentrations of the lysate from microdissected vessels, tubules and glomeruli were measured using a Bio-Rad protein assay kit according to the microassay procedures as we described previously (Wu *et al.,* 1999).

HPLC analysis of cADPR and ADPR. To determine the activity of ADP-ribosyl cyclase, the homogenate (10 μg) prepared from bulk-dissected renal vessels and the lysates from microdissected renal microvessels or VSMCs were incubated with 1 mM nicotinamide guanine dinucleotide (NGD) at 37°C for 30 min in Hepes buffer (pH 7.4). NGD was used as a substrate to determine ADP-ribosyl cyclase activity, because this enzyme converts NGD into cGDPR, but unlike cADPR, cGDPR may not be hydrolyzed by cADPR hydrolase (Graeff *et al.,* 1994). Therefore, the conversion rate of NGD into cGDPR more accurately represented the activity of ADP-ribosyl cyclase in the tissue. The reaction was terminated by removal of protein from the reaction mixtures with Microcon-30 ultrafilter (AMICON) by centrifuging at 3000*g* at 4°C.

A fluorescent product of ADP-ribosyl cyclase, cGDPR was separated by HPLC and detected with a Hewlett Packard 1046A fluorometer. The excitation wavelength was set at 300 nm, and the emission wavelength was 410 nm.

To determine the hydrolysis of cADPR, the homogenates or lysates of renal vessels were incubated with 1 mM cADPR at 37°C for 30 min, and the products were chromatographed and analyzed using a Hewlett Packard HPLC system with a 1040A photodiode array detector. The column effluent was monitored at 254 nm.

The HPLC system consisted of two Model 110B solvent delivery modules, a 421A controller (Beckman, Berkeley, CA), and a 1040A photodiode array detector or a fluorometric detector with a 20-μl flow cell (Hewlett Packard, Avondale, PA). Nucleotides were separated and analyzed in a 3-μm Supelcosil LC-18 column (4.6 $\times$ 150 mm) with a 5-μm Supelcosil LC-18 (4.6 $\times$ 20-mm) guard column (Supelco, Bellefonte, BA). The injection volume was 20 μl. For cGDPR, the mobile phase consisted of 0.15 M ammonium acetate (pH 5.5) containing 5% methanol (Buffer A) or 50% methanol (Buffer B). For ADPR, the mobile phase consisted of 10 mM potassium dihydrogen phosphate (pH 5.5) containing 5 mM tetrabutylammonium dihydrogen sulfate and 5% acetonitrile (buffer A) and 50% acetonitrile (buffer B). The gradient started from 5% of buffer B, to 30% of buffer B in 25 min, and then up to 50% buffer B in 1 min and continued for 9 min. The flow rate was 0.8 ml/min. The chromatogram was monitored using a fluorescence detector or UV detector as indicated above. Peak identities were confirmed by the retention times and absorption spectra (taken during the peak elution) as compared to the synthetic standards. Data were collected and analyzed by a Chemstation (Hewlett-Packard). Quantitative measurements were performed by comparison of known concentration of standards. All these HPLC methods and protocols were validated in our previous studies (Geiger *et al.*, 2000; Li *et al.*, 1998; Yu *et al.*, 1998).

$[Ca^{2+}]_i$ assay in renal arterial smooth muscle cells. Arterial smooth muscle cells were enzymatically dissociated from microdissected renal interlobular and afferent arterioles (<100 μm) as we described previously (Zou *et al.*, 1996a,b). A calcium-sensitive fluorophore, fura 2-AM (Molecular Probes, Eugene, OR) was used for monitoring $[Ca^{2+}]_i$ (Tsien, 1989). Freshly dissociated renal arterial smooth muscle cells on poly-d-lysine-coated glass coverslips were washed using Hanks' buffer, which contains (mM): NaCl, 130; KCl, 5.4; Hepes, 5.5; Glucose, 5.5; $CaCl_2$, 1.25; and $MgCl_2$, 1; and incubated with 5 μM fura 2-AM at 37°C for 30 min. The coverslip was mounted on a perfusion chamber and then on the stage of an inverted microscope (Nikon Diaphot). The cells were incubated with Hanks' buffer for 20 min at room temperature to allow for complete deesterification of intracellular fura-2, and the ratio of fura-2 emissions when excited at 340 and 380 nm (F_{340}/F_{380}) was monitored by using a fluorescence microscopic spectrometry system (PTI). $[Ca^{2+}]_i$ was calculated using $[Ca^{2+}]_i$ (nM) = $K_d \times (F_O/F_S) \times (R - R_{min})/(R_{max} - R)$, where R is the ratio of F_{340}/F_{380}. K_d is a dissociation constant. R_{min} and R_{max} are minimal and maximal ratio of F_{340}/F_{380}, respectively; F_O and F_S represent the maximal and minimal signal intensity at 380 nm, respectively. K_d was 224 nM. R_{max} was calculated from the fluorescence intensity after permeabilizing the cells with 5 μM ionomycin and represented maximal $[Ca^{2+}]_i$. R_{min} was obtained by addition of 2 mM EGTA and represented the minimal $[Ca^{2+}]_i$ (Cornfield *et al.*, 1994; Tsien, 1989).

Direct measurement of calcium release from sarcoplasmic reticulum (SR). Renal arterial smooth muscle cells on coverslips were first equilibrated with Hanks' buffer for 20 min and then washed and incubated with 5 μM fura-2-AM at 37°C for 30 min. The coverslip was mounted on a perfusion chamber and then on the stage of an inverted microscope. The cells were permeabilized with 10 μM β-escin for 3–5 min in a pCa 9.0 solution and washed for 2 min to remove β-escin as described previously (Kannan *et al.*, 1996; Yu *et al.*, 1998). Permeabilized cells were incubated with pCa 6.0 solution for 10–20 min to load Ca^{2+} into the SR. Using a fluorescence microscopic spectrometry system, SR Ca^{2+} release was monitored when cADPR (10 μM, Calbiochem, CA) was added. To examine the effect of CICR inhibition on cADPR-induced Ca^{2+} release response, tetracaine (20 μM) was used to pretreat the cells. Doses for cADPR and tetracaine used in the present study were demonstrated to effectively alter Ca^{2+} release in other tissues by previous studies in our

laboratory and by others (Csernoch *et al.*, 1999; Kannan *et al.*, 1996; Yu *et al.*, 1998; Overend *et al.*, 1997). The fluorescence intensity of intracellular fura-2 was determined and recorded when excited at 340 and 380 nm, and Ca^{2+} release was indicated by the ratio of F_{340}/F_{380}. This Ca^{2+} release response to cADPR was confirmed to be IP_3 independent, since it was blocked by cADPR antagonist, 8-Br-cADPR, but not by IP_3 antagonist, heparin (Yu *et al.*, 1998; Li *et al.*, 2000). As the cells were permeabilized, intracellular $[Ca^{2+}]$ might not be calculated (Kannan *et al.*, 1996).

Isolated and perfused renal arterial preparation. Small renal interlobular arteries (100–150 μm, i.d.) from Sprague–Dawley rats were carefully dissected and stored in ice-cold PSS. Segments of small arteries were mounted on glass pipettes in a water-jacketed perfusion chamber. The small arteries were perfused and bathed with PSS that was equilibrated with a 95% O_2–5% CO_2 mixture and maintained at 37°C. This arterial preparation has been shown to have an intact endothelium (Geiger *et al.*, 2000; Zou *et al.*, 1996a; Li *et al.*, 1999). In the present study, we did not check the integrity of the endothelium in each experiment. However, in previous studies and our recent experiments about endothelium-dependent vasodilation, 95% arteries can be isolated and mounted with an intact endothelium, as determined by a vasodilator response to bradykinin (data not shown). After mounting the artery, the outflow cannula was clamped, and the artery was pressurized to 80 mmHg and equilibrated for 1.5 h. Internal diameter of the artery was measured using a video system composed of a stereomicroscope (Leica MZ8, Leica, Switzerland), a CCD camera (KP-MI AU, Hitachi, Japan), a video monitor (VM-1221, Hitachi, Japan), a video measuring apparatus (VIA-170, Boeckeler Instrument, Tucson, AR) and a video printer (UP890 MD, Sony, Japan). The arterial images were recorded continuously with a video cassette recorder (M-674, Toshiba, Japan). The effects of cADPR on arterial diameters were studied by cumulative additions of cADPR (0.1–10 μM) into the bath solution.

Statistics. Data are presented as means ± 1 S.E. The significance of differences within and between groups for multiple groups of data was evaluated using an two-way ANOVA followed by a postdoc test (Duncan's multiple range test) and for two groups of data using a Student's *t* test (SigmaStat, San Rafael, CA). $P < 0.05$ was considered statistically significant.

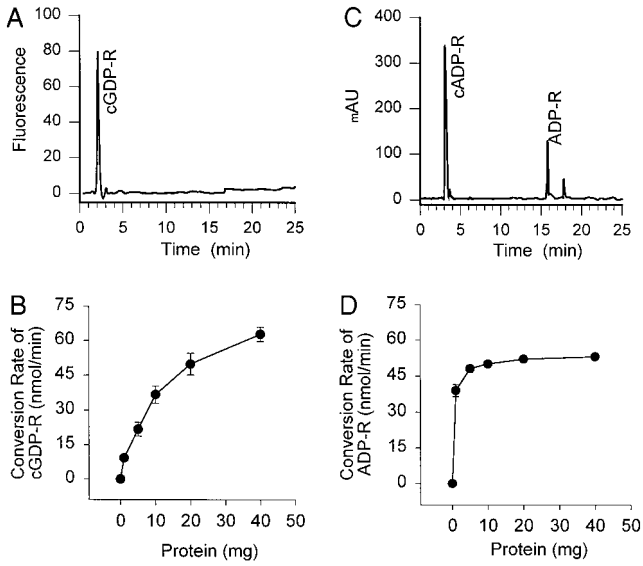

FIG. 1. Production and hydrolysis of cADPR in the homogenates of renal preglomerular arteries. (A) A representative HPLC chromatogram depicting the conversion of NGD into cGDP-ribose by the homogenates, which represents the activity of ADP-ribosyl cyclase. (B) Summarized data showing the conversion rates of NGD into cGDP-ribose in a protein concentration-dependent manner ($n = 7$ rats). (C) A representative UV HPLC chromatogram depicting the conversion of cADPR into ADPR, which represents the activity of cADPR hydrolase. (D) Summarized data showing the conversion rates of cADPR into ADPR ($n = 5$ rats).

RESULTS

Production and hydrolysis of cADPR in the homogenate prepared from intrarenal arteries. Figure 1A shows a representative fluorescent reverse phase-HPLC chromatogram depicting the conversion of NGD into cGDPR in the homogenates of renal arteries. The conversion rate of NGD into cGDPR represented the ADP-ribosyl cyclase activity. Fluorescent cGDPR had a retention time of 2.1 min. As shown in Fig. 1B, the conversion rate of NGD into cGDPR was increased with elevated protein concentrations in the reaction mixtures. The maximal conversion rate of NGD into

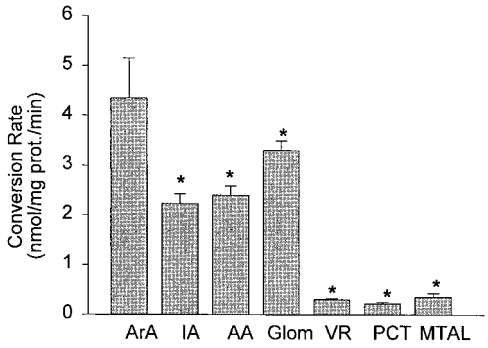

FIG. 2. ADP-ribosyl cyclase activity in the lysate or homogenates of microdissected renal vessels and tubules. These vessel and tubule segments included arcuate artery (ArA, $n = 6$ rats), interlobular artery (IA, $n = 6$), afferent arteriole (AA, $n = 7$), vasa recta (VR, $n = 10$), proximal convoluted tubule (PCT, $n = 6$), medullary collecting duct (mTAL, $n = 6$), and glomeruli (Glm, $n = 10$). *Indicates significant difference ($P < 0.05$) compared with the values obtained from ArA.

cGDPR averaged 8.69 ± 2.39 nmol/min/mg protein in these vessels. The degradation product of cADPR, ADPR, was analyzed by HPLC with a UV detector. A representative chromatogram is presented in Fig. 1C. cADPR and ADPR had retention times of 3.1 and 15.8 min, respectively. A protein concentration-dependent increase in the cADPR hydrolase activity was observed when cADPR was incubated with renal arterial homogenate (Fig. 1D).

Production of cADPR in microdissected renal microvessels. Compared to the tubule segments (proximal convoluted tubule (PCT) and medullary thick ascending limb (mTAL)), the renal vessels, including microvessels such as interlobular and afferent arterioles, expressed greater ADP-ribosyl cyclase activity. Maximal enzyme activity was found in arcuate arteries. The enzyme activity was much higher in afferent arterioles than in vasa recta. Glomeruli also produced cADPR, and the enzyme activity in glomeruli was similar to the preglomerular arteries and arterioles (Fig. 2).

Production of cADPR in renal arterial SMCs. When the lysate of renal vascular SMCs was incubated with 1 mM NGD, the conversion rate of NGD into cGDPR was increased in a protein concentration-dependent manner. The relationship between the production of cADPR and protein concentrations in renal vascular SMCs was similar to that in renal arterial homogenate. The maximal conversion rate of NGD into cGDPR averaged 10.97 ± 2.39 nmol/min/mg protein in these SMCs (Fig. 3).

Effect of cADPR on Ca^{2+} release and intracellular $[Ca^{2+}]$ in renal arterial SMCs. Figure 4A presents a typical recording depicting Ca^{2+} release response from the SR of β-escin-permeabilized renal arterial smooth muscle cells and the effect of the CICR inhibitor, tetracaine on the SR Ca^{2+} release induced by cADPR. Addition of cADPR (10 μM) produced a rapid Ca^{2+} release response. In the presence of tetracaine (20 μM), the effect of cADPR on the SR Ca^{2+} release was substantially attenuated. Figure 4B summarizes the Ca^{2+} release response to cADPR in the absence and presence of tetracaine. cADPR increased the ratio of F_{340}/F_{380} by 0.53, a 75% increase. In the presence of tetracaine, cADPR-induced Ca^{2+} release was reduced by 70%.

In fura-2-loaded cells without β-escin-permeabilization, cADPR increased $[Ca^{2+}]_i$ from baseline of 238 to 283 nM, which represents a mild increase in $[Ca^{2+}]_i$ compared to the permeabilized cells. In contrast to a rapid Ca^{2+} response in the β-escin-permeabilized cells, increase in $[Ca^{2+}]_i$ in these intact cells occurred 10–15 min after cADPR was added into the bath. Ca^{2+} channel blocker, nifedipine (10 μM) had no effect on cADPR-induced increase in $[Ca^{2+}]_i$. In the presence of tetracaine (20 μM), cADPR only elevated $[Ca^{2+}]_i$ from 172 to 189 nM. The Ca^{2+} response of tetracaine-pretreated cells to cADPR was reduced by 62%.

Effect of cADPR on renal arterial diameters. Addition of cADPR into the bath solution produced

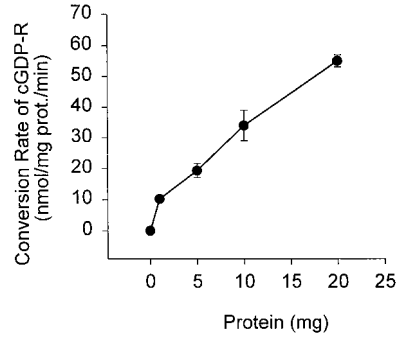

FIG. 3. ADP-ribosyl cyclase activity in renal arterial smooth muscle cells ($n = 6$ rats). The cells were enzymatically dissociated from renal interlobular and afferent arterioles.

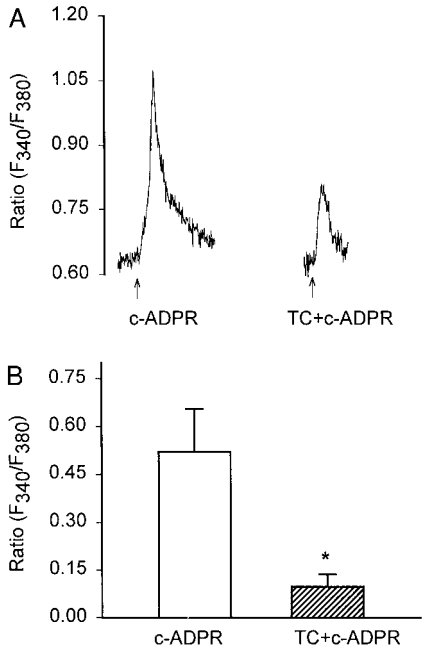

FIG. 4. Ca^{2+} release from sarcoplasmic reticulum (SR) in β-escin-permeabilized renal arterial smooth muscle cells. (A) Representative recordings of Ca^{2+} release from the SR in response to cADP-R (10 μM) in the absence or presence of CICR inhibitor, tetracaine (20 μM). Ca^{2+} release was indicated by a ratio of fura-2 fluorescence at 340 and 380 (F_{340}/F_{380}) measured using the fluorescent microscopic spectrometry. (B) Summarized data showing cADPR-induced Ca^{2+} release in (Δ ratio (F_{340}/F_{380}) the absence or presence of tetracaine ($n = 6$ rats). *Indicates significant difference ($P < 0.05$) compared with the values in the absence of tetracaine.

time-dependent vasoconstriction. The decrease in arterial diameter reached a plateau 25 min after administration of cADPR. The typical video images of isolated, perfused, and pressurized renal interlobular artery are presented in Fig. 5A. The diameter of this pressurized renal artery was markedly reduced 25 min after cADPR (10 μM) was added into the bath, suggesting a vasoconstriction. Pretreatment of the renal artery with tetracaine (20 μM) blocked the vasoconstrictor effect of cADPR. Figure 5B summarizes the effects of cADPR on vascular diameter of small renal arteries. Addition of cADPR into the bath produced a concentration-dependent decrease in vascular diameter. The vasoconstrictor effect of cADPR can be completely blocked by tetracaine.

DISCUSSION

In the present study, the enzymatic pathway responsible for the production and metabolism of a novel Ca^{2+} mobilizing second messenger, cADPR was characterized in the renal vasculature. Using HPLC analysis, we demonstrated that the homogenate pre-

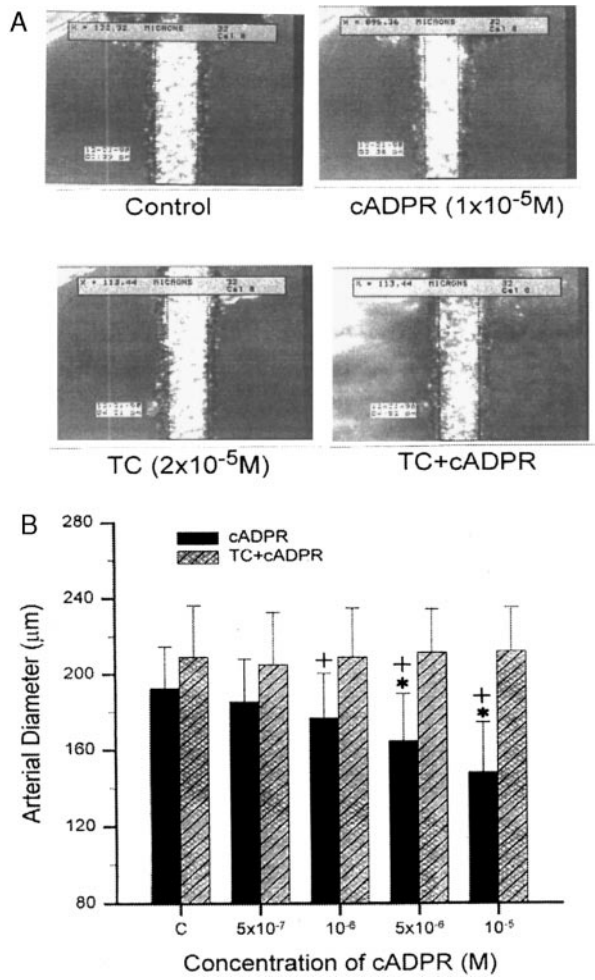

FIG. 5. Effect of cADPR on the diameter of renal interlobular arteries. (A) Representative video prints of a renal interlobular artery before and after addition of cADPR and/or tetracaine into the bath solution. (B) Summarized data showing the effects of cADPR on the diameters of renal interlobular arteries in the absence and presence of tetracaine ($n = 8$ rats). *Indicates significant difference ($P < 0.05$) compared with control, and + indicates significant difference compared with the values obtained before addition of tetracaine.

pared from preglomerular arteries expressed the activity of ADP-ribosyl cyclase and cADPR hydrolase, suggesting that cADPR is produced and hydrolyzed in these blood vessels. Recent studies have indicated that in a variety of mammalian tissues NAD is converted into cADPR by cyclization via ADP-ribosyl cyclase and cADPR can be hydrolyzed by cADPR hydrolase. The activities of both enzymes determine cADPR concentrations within cells and thereby control intracellular Ca^{2+} mobilization (Beer *et al.*, 1995b; Galione *et al.*, 1993; Koshiyama *et al.*, 1991; Lee, 1994; Lee and Aarhus, 1993; Takasawa *et al.*, 1993; White *et al.*, 1993). Therefore, demonstration of ADP-ribosyl cyclase and cADPR hydrolase in the renal vasculature suggests the presence of cADPR-mediated Ca^{2+} signaling pathway.

To determine the localization of cADPR production, renal microvessels and tubules were microdissected along the renal nephron for the analysis of ADP-ribosyl cyclase activity. In the pre- and postglomerular microvessels including afferent arterioles and vasa recta, the production of cADPR was detected. Preglomerular arteries or arterioles exhibited a greater activity of ADP-ribosyl cyclase compared to postglomerular vasa recta. In tubule segments such as proximal convoluted tubules and medullary thick ascending limb, ADP-ribosyl cyclase activity was minimal. It appears that the vascular smooth muscle expressed great activity of ADP-ribosyl cyclase since preglomerular arteries have more smooth muscle cells compared to vasa recta and tubule segments. This view is supported by a direct measurement of cADPR production in arterial smooth muscle cells dissociated from interlobular and afferent arterioles. The activity of ADP-ribosyl cyclase was found to be comparable in these arterial smooth muscle cells to whole vascular homogenates. In previous studies, we also demonstrated that cultured coronary vascular smooth muscle cells produced more cADPR compared to endothelial cells (Li *et al.*, 1998; Yu *et al.*, 1998). Given the role that cADPR plays in the control of intracellular Ca^{2+} mobilization, enriched ADP-ribosyl cyclase activity in vascular smooth muscle cells may be of importance in the control of vascular tone in renal arteries or arterioles through cADPR-mediated action on $[Ca^{2+}]_i$.

To test this hypothesis, we determined the effects of cADPR to stimulate Ca^{2+} release from intracellular stores and to increase $[Ca^{2+}]_i$ in single vascular smooth muscle cells with the use of fluorescent microscopic spectrometry. Using β-escin permeabilized arterial smooth muscle cells isolated from renal interlobular and afferent arterioles, the direct action of cADPR to stimulate Ca^{2+} release was observed. As described in previous studies using β-escin permeabilized porcine coronary arterial smooth muscle cells, a rapid increase in Ca^{2+} signal induced by cADPR represents Ca^{2+} release from the sarcoplasmic reticulum (Kannan *et al.*, 1996). Since IP_3 receptor inhibitor, heparin had no effect on this Ca^{2+} release response, it seems that the effect of cADPR is not associated with IP_3 signaling pathway in these vascular smooth muscle cells. This is in agreement with other reports indicating that cADPR mobilizes intracellular Ca^{2+} through a mechanism independent of IP_3 (Lee, 1993, 1994; Lee *et al.*, 1994).

The present study also explored the mechanism by which cADPR stimulates Ca^{2+} release from sarcoplasmic reticulum in renal arterial smooth muscle cells. There is accumulating evidence indicating that cADPR may mobilize intracellular Ca^{2+} through Ca^{2+}-induced Ca^{2+} release (CICR) in nonvascular tissues. It has been demonstrated that procaine and ruthenium red, the CICR blockers selectively inhibit the cADPR-induced Ca^{2+} release and that caffeine and Ca^{2+} as the agonists of CICR dramatically potentiated Ca^{2+}-releasing activity of cADPR (Galione *et al.*, 1991; Lee, 1993, 1994). In the present study, tetracaine, a specific CICR inhibitor (Csernoch *et al.*, 1999; Overend *et al.*, 1997) was used to address the association of CICR with cADPR-induced Ca^{2+} release. The results showed that in β-escin-permeabilized renal arterial smooth muscle cells tetracaine markedly decreased cADPR-induced Ca^{2+} release response, suggesting that CICR contributes to the actions of cADPR in these arterial smooth muscle cells.

cADPR-sensitive CICR has been shown to play an important role in excitation–contraction coupling in cardiac muscle and in the coupling between Ca^{2+} influx and intracellular Ca^{2+} release in the neurons (Empson and Galione, 1997; Galione *et al.*, 1998; Rakovic *et al.*, 1996). In vascular smooth muscle, CICR may also participate in the regulation of intracellular

$[Ca^{2+}]$ and vascular tone (Berridge, 1997; Ito *et al.*, 1991; Kamishima and McCarron, 1997; Knot *et al.*, 1998). It has been indicated that under the resting condition, $[Ca^{2+}]_i$ in vascular smooth muscle cells is dependent on Ca^{2+} influx, spontaneous brief Ca^{2+} releasing bursts from the sarcoplasmic reticulum and CICR. Alteration of either Ca^{2+} influx or intracellular Ca^{2+} release would change the resting Ca^{2+} levels and vascular tone (Berridge, 1997). In addition, the entry of Ca^{2+} through voltage-operating channels may be amplified by CICR, resulting in a global Ca^{2+} increase throughout the cytoplasma and nucleus and consequently producing vasoconstriction (Berridge, 1994, 1997). Considering the association of cADPR and CICR, we propose that cADPR may play a critical role in the control of the resting tone and in the development of vasoconstriction induced by different stimuli such as activation of voltage-operating Ca^{2+} channels in the renal arteries or arterioles.

Using isolated, perfused and pressurized renal interlobular arterial preparation, cADPR was found to decrease arterial diameters when added into the bath solution, suggesting a vasoconstrictor response to this nucleotide. Since cADPR has been considered as an intracellular second messenger, it remains unknown how this nucleotide produces vasoconstriction and how it enters into the cells when administrated exogenously. However, there are three lines of evidence indicating that cADPR induces vasoconstriction in this arterial preparation through increases in $[Ca^{2+}]_i$ or CICR mechanism. First, cADPR was found to increase $[Ca^{2+}]_i$ in intact arterial smooth muscle cells when added into the bath solution by direct measurement with the single cell fluorescent spectrometry. The increase in intracellular Ca^{2+} may activate arterial vasoconstriction. Second, tetracaine, a CICR inhibitor substantially blocked the increase in $[Ca^{2+}]_i$ and vasoconstrictor response to exogenously administrated cADPR. This suggests that the vasoconstrictor effect of cADPR is associated with CICR mechanism. Finally, a time delay of both increase in intracellular Ca^{2+} response and vasoconstriction was observed when cADPR was added into the bath solution, suggesting that a time period is needed for cADPR to enter into the cells. In regard to the mechanism by which cADPR enters into the cells, recent studies indicated that the NAD/cADPR transporters on the cell membrane may mediate the uptake of these nucleotides (Zocchi *et al.*, 1999). However, the physiological significance of this cADPR transport system in intracellular Ca^{2+} signaling remains to be further elucidated.

In summary, we demonstrate that vascular smooth muscle in renal vasculature, including afferent arterioles and vasa recta, is capable to produce and hydrolyze cADPR. cADPR stimulates Ca^{2+} release from the sarcoplasmic reticulum of vascular smooth muscle cells and thereby produces renal vasoconstriction through CICR mechanism. We conclude that an enzymatic pathway for cADPR production and metabolism is present in renal vascular smooth muscle and that cADPR-mediated Ca^{2+} signaling may importantly contribute to the control of renal vascular tone through CICR.

ACKNOWLEDGMENTS

This study was supported by NIH Grants HL-57244 (P.L.L.) and DK-54927 (A.P.Z.) and American Heart Association, Grant-In-Aid 96007310 (A.P.Z.).

REFERENCES

Beers, K. W., Chini, E. N., and Dousa, T. P. (1995a). All-*trans*-retinoic acid stimulates synthesis of cyclic ADP-ribose in renal LLC-PK1 cells. *J. Clin. Invest.* **95,** 2395–2390.

Beers, K. W., Chini, E. N., Lee, H. C., and Dousa, T. P. (1995b). Metabolism of cyclic ADP-ribose in opossum kidney renal epithelial cells. *Am. J. Physiol.* **268** (*Cell Physiol.* **37**), C741–C746.

Berridge, M. J. (1994). The biology and medicine of calcium signaling. *Mol. Cell. Endocrinol.* **98,** 119–124.

Berridge, M. J. (1997). Elementary and global aspects of calcium signalling. *J. Physiol.* **499** (Pt. 2), 291–306.

Chini, E. N., Toledo, F. G., Thompson, M. A., and Dousa, T. P. (1997). Effect of estrogen upon cyclic ADP ribose metabolism: β-Estradiol stimulates ADP ribosyl cyclase in rat uterus. *Proc. Natl. Acad. Sci. USA* **94,** 5872–5876.

Chini, E. N., Beers, K. W., Chini, C. S., and Dousa, T. P. (1995). Specific modulation of cyclic ADP-ribose-induced Ca^{2+} release by polyamines. *Am. J. Physiol.* **269,** C1042–C1047.

Cornfield, D. N., Stevens, T., McMurtry, I. F., Abman, S. H., and Rodman, D. M. (1994). Acute hypoxia causes membrane depolarization and calcium influx in fetal pulmonary artery smooth muscle cells. *Am. J. Physiol.* **266**(10), L469–L475.

Csernoch, L., Szentesi, P., Sarkozi, S., Szegedi, C., Jona, I., and Kovacs, L. (1999). Effects of tetracaine on sarcoplasmic calcium release in mammalian skeletal muscle fibres. *J. Physiol.* **515** (Pt. 3), 843–857.

de Toledo, F. G., Cheng, J., and Dousa, T. P. (1997). Retinoic acid and triiodothyronine stimulate ADP-ribosyl cyclase activity in rat vascular smooth muscle cells. *Biochem. Biophys. Res. Commun.* **238,** 847–850.

Empson, R. M., and Galione, A. (1997). Cyclic ADP-ribose enhances coupling between voltage-gated Ca^{2+} entry and intracellular Ca^{2+} release. *J. Biol. Chem.* **272,** 20967–20970.

Geiger, J., Zou, A. P., Campbell, W. B., and Li, P. L. (2000). Inhibition of cyclic ADP-ribose formation produces vasorelaxation in bovine coronary arteries. *Hypertension* **35,** 397–402.

Galione, A., Lee, H. C., and Busa, W. B. (1991). Ca^{2+}-induced Ca^{2+} release in sea urchin egg homo genates and its modulation by cyclic ADP-ribose. *Science* **253,** 1143–1146.

Galione, A. (1993). Cyclic ADP-ribose: A new way to control calcium. *Science* **259,** 325–326.

Galione, A., White, H., Willmott, N., Turner, M., Potter, B. V. L., and Watson, S. P. (1993). cGMP mobilizes intracellular Ca^{2+} in sea urchin eggs by stimulating cyclic ADP-ribose synthesis. *Nature* **365,** 456–459.

Galione, A., Cui, Y., Empson, R., Iino, S., Wilson, H., and Terrar, D. (1998). Cyclic ADP-ribose and the regulation of calcium-induced calcium release in eggs and cardiac myocytes. *Cell Biochem. Biophys.* **28,** 19–30.

Graeff, R. M., Walseth, T. F., Fryxell, K., Branton, W. D., and Lee, H. C. (1994). Enzymatic synthesis and characterizations of cyclic GDP-ribose. *J. Biol. Chem.* **269,** 30260–30267.

Howard, M., Grimaldi, J. C., Bazan, J. F., Lund, F. E., Santos-Argumedo, L., Parkhouse, R. M. E., Walseth, T. F., Lee, H. C. (1993). Formation and hydrolysis of cyclic ADP-ribose catalysed by lymphocyte antigen CD38. *Science* **262,** 1056–1059.

Ito, K., Ikemoto, T., and Takakura, S. (1991). Involvement of Ca^{2+} influx-induced Ca^{2+} release in contractions of intact vascular smooth muscles. *Am. J. Physiol.* **261,** H1464–H1470.

Kamishima, T., and McCarron, J. G. (1997). Regulation of the cytosolic Ca^{2+} concentration by Ca^{2+} stores in single smooth muscle cells from rat cerebral arteries. *J. Physiol.* **501** (Pt. 3), 497–508.

Kannan, M. S., Fenton, A. M., Prakash, Y. S., and Sieck, G. C. (1996). Cyclic ADP-ribose stimulates sarcoplasmic reticulum calcium release in porcine coronary artery smooth muscle. *Am. J. Physiol.* **270** (*Heart Circ. Physiol.* **39**), H801–H806.

Knot, H. J., Standen, N. B., and Nelson, M. T. (1998). Ryanodine receptors regulate arterial diameter and wall [Ca^{2+}] in cerebral arteries of rat via Ca^{2+}-dependent K^+ channels. *J. Physiol.* **508,** 211–221.

Koguma, T., Takasawa, S., Tohgo, A., Karasawa, T., Furuya, Y., Yonekura, H., and Okamoto, H. (1994). Cloning and characterization of cDNA encoding rat ADP-ribosyl cyclase/cyclic ADP-ribose (homologue to human CD38) from islets of langerhans. *Biochim. Biophys. Acta* **1223,** 160–162.

Koshiyama, H. H., Lee, H. C., and Tashjian, A. H. (1991). Novel mechanisms of intracellular calcium release in pituitary cell. *J. Biol. Chem.* **266,** 16985–16988.

Lee, H. C. (1993). Potentiation of calcium- and caffeine-induced calcium release by cyclic ADP-ribose. *J. Biol. Chem.* **268,** 293–299.

Lee, H. C. (1994). A signaling pathway involving cyclic ADP-ribose, cGMP, and nitric oxide. *NIPS* **9,** 134–137.

Lee, H. C., and Aarhus, R. (1993). Wide distribution of an enzyme that catalyzes the hydrolysis of cyclic ADP-ribose. *Biochim. Biophys. Acta* **1164,** 68–74.

Lee, H. C., Aarhus, R., Graeff, R., Gurnack, M. E., and Walseth, T. F. (1994b). Cyclic ADP ribose activation of the ryanodine receptor is mediated by calmodulin. *Nature* **370,** 307–309.

Lee, H. C., Walseth, T. F., Bratt, G. T., Hayes, R. N., and Clapper, D. L. (1989). Structural determination of a cyclic metabolite of NAD+ with intracellular Ca^{2+} mobilizing activity. *J. Biol. Chem.* **264,** 1608–1615.

Li, P.-L., Zou, A. P., and Campbell, W. B. (1998). Regulation of the K_{Ca} channel activity by cyclic ADP-ribose and ADP-ribose in bovine coronary arterial smooth muscle. *Am. J. Physiol.* **275,** H1002–H1010.

Li, P.-L., Zhang, D. Z., Zou, A. P., and Campbell, W. B. (1999). Effects of ceramide, a sphingomyelin metabolite, on the K_{Ca} channel activity. *Hypertension* **33,** 1441–1446.

Li, N., Teggatz, E. G., Li, P.-L., Campbell, W. B., and Zou, A. P. (2000). Cyclic ADP-ribose-mediated Ca^{2+} signaling and Ca^{2+}-induced Ca^{2+} release in preglomerular arterial smooth muscle cells. *FASEB J.* **14,** A130. [Abstract]

Morita, K., Kitayama, S., and Dohi, T. (1997). Stimulation of cyclic ADP-ribose synthesis by acetylcholine and its role in catecholamine release in bovine adrenal chromaffin cells. *J. Biol. Chem.* **272,** 21002–21009.

Overend, C. L., Eisner, D. A., and O'Neill, S. C. (1997). The effect of tetracaine on spontaneous Ca^{2+} release and sarcoplasmic reticulum calcium content in rat ventricular myocytes. *J. Physiol.* **502:** (Pt. 3), 471–479.

Rakovic, S., Galione, A., Ashamu, G. A., Ptter, B. V. L., and Terrar, D. A. (1996). A specific cyclic ADP-ribose antagonist inhibits cardiac excitation-contraction coupling. *Curr. Biol.* **6,** 989–996.

Shubinsky, G., and Schlesinger, M. (1997). The CD38 lymphocyte differentiation marker: New insight into its ectoenzymatic activity and its role as a signal transducer. *Immunity* **7**(3), 315–324.

States, D. J., Walseth, T. F., and Lee, H. C. (1992). Similarities in amino acid sequences of *Aplysia* ADP-ribosyl cyclase and human lymphocytes antigen CD38. *Trends Biochem. Sci.* **17,** 495–599.

Takesawa, S., Nata, K., Yonekura, H., and Okamoto, H. (1993). Cyclic ADP-ribose in insulin secretion from pancreatic cells. *Science* **259,** 370–373.

Tanaka, Y., and Tashjian, A. H., Jr. (1995). Calmodulin is a selective mediator of Ca^{2+}-induced Ca^{2+} release via the ryanodine recep-

tor-like Ca^{2+} channel triggered by cyclic ADP-ribose. *Proc. Natl. Acad. Sci. USA* **92,** 3244–3248.

Tsien, R. Y. (1989). Fluorescent probes of cell signaling. *Annu. Rev. Neurosci.* **12,** 227–253.

Ullmer, C., Boddeke, H. G., Schmuck, K., and Lubbert, H. (1996). 5-HT2B receptor-mediated calcium release from ryanodine-sensitive intracellular store in human pulmonary artery endothelial cells. *Br. J. Pharmacol.* **117,** 1081–1088.

White, A. M., Watson, S. P., and Galione, A. (1993). Cyclic ADP-ribose-induced Ca^{2+} release from rat brain microsomes. *FEBS Lett.* **318,** 259–263.

Wu, F., Li, P. L., and Zou, A. P. (1999). Microassay of 5′-nucleotidase and adenosine deaminase activity in microdissected nephron segments. *Anal. Biochem.* **266,** 133–139.

Yu, J.-Z., Zou, A. P., Compbell, W. B., Li, P.-L. (1998). Role of cyclic ADP-ribose in NO-induced decrease in intracellular calcium in coronary smooth muscle cells. *FASEB J.* **12,** A406 (abstract).

Zocchi, E., Usai, C., Guida, L., Franco, L., Bruzzone, S., Passalacqua, M., and de Flora, A. (1999). Ligand-induced internalization of CD38 results in intracellular Ca^{2+} mobilization: Role of NAD^{+} transport across cell membranes. *FASEB J.* **13,** 273–283.

Zou, A. P., Fleming, J. T., Falck, J. R., Jacobs, E. R., Gebremedhin, D., Harder, H. D., and Roman, R. J. (1996). 20-Hydroxyeicosatetraenoic acid is an endogenous inhibitor of calcium-activated large conductance K^{+} channels in renal arterioles. *Am. J. Physiol.* **270,** (*Reg. Interg. Com. Physiol.* **39**), R228–R237.

Zou, A. P., Fleming, J. T., Falck, J. R., Jacobs, E. R., Gebremedhin, D., Harder, D. R., and Roman, R. J. (1996). Stereospecific effect of 11,12-Epoxyeicosatrienoic acid on vascular tone and K^{+}-channel activity of renal arterioles in rats. *Am. J. Physiol.* **270** (*Renal Fluid Electrolyte Physiol.* **39**), F822–F832.